Geological Circular 78-6

Identification of Surface Faults by Horizontal Resistivity Profiles

TEXAS COASTAL ZONE

Bureau of Economic Geology • W. L. Fisher, Director • The University of Texas at Austin • Austin, Texas 78712

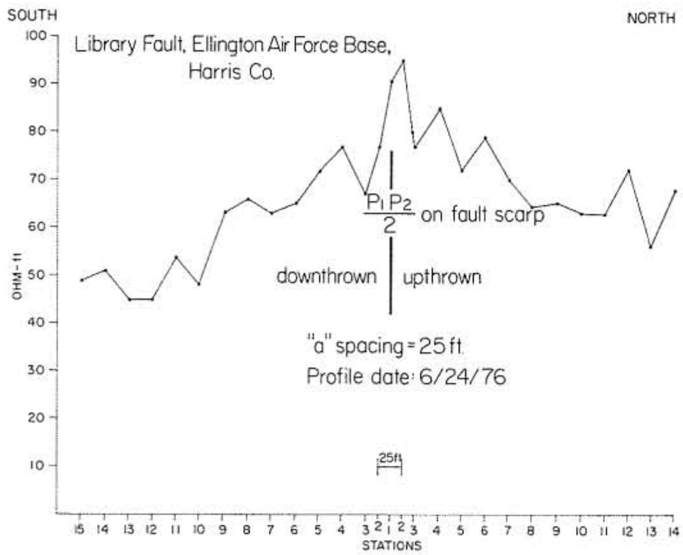

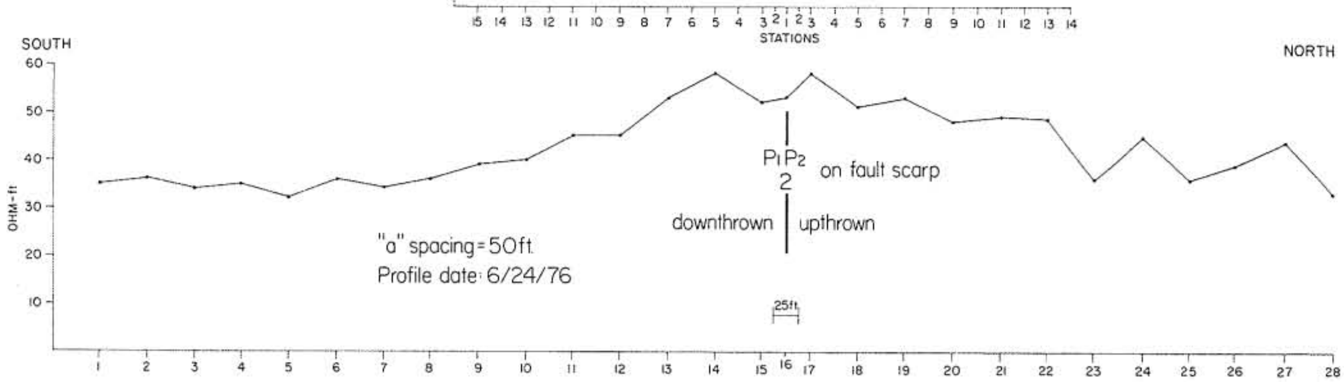

by Charles W. Kreitler and Dawn G. McKalips

1978

Second Printing, September 1982

Geological Circular 78-6

IDENTIFICATION OF SURFACE FAULTS BY HORIZONTAL RESISTIVITY PROFILES, TEXAS COASTAL ZONE

by

Charles W. Kreitler and Dawn G. McKalips

Sponsored by
U. S. Geological Survey, Department of Interior
Grant No. 14-08-0001-G144

Bureau of Economic Geology
The University of Texas at Austin
Austin, Texas 78712
W. L. Fisher, Director

CONTENTS

FIGURES

IDENTIFICATION OF SURFACE FAULTS BY HORIZONTAL RESISTIVITY PROFILES, TEXAS COASTAL ZONE

by Charles W. Kreitler and Dawn G. McKalips

INTRODUCTION

The land surface in the Texas Coastal Zone is interlaced with active and potentially active surface faults. They are subtle features which are difficult to identify until they have caused damage to manmade structures. To date (1978), significant damage has resulted. Faults intercept 2 airports, interstate highways at 11 different locations, and railroad tracks at 28 locations. Faults also pass through 11 residential communities. More than 200 houses in these communities in Harris and Galveston Counties show structural damage because of faulting (fig. 1). Fault movements of only a few inches per decade can cause significant structural damage, and no architectural style or structural design is immune. Foundations break, and cracks extend up the exterior and interior walls of the structure. Although breaks in buildings and highways are one of the best criteria for identifying surface faults, the damage has already occurred.

Kreitler (1976) has listed four criteria that can be used to identify the presence of a surface fault before a structure is built. They are recognition of (1) topographic scarps; (2) shallow subsurface faults, using electrical logs or other geophysical data and subsequently extrapolating the fault to land surface; (3) shallow subsurface faults, by coring or trenching; and (4) the surface trace of lineations observed on a fault (lineation), using black-and-white, color, and color-infrared aerial photographs or other remote sensing techniques. This paper presents and evaluates another technique for the detection of surface faults--the use of horizontal electrical resistivity profiling.

In the Texas Coastal Zone, similar surficial geology commonly occurs on both sides of a fault. Furthermore, shallow subsurface fault displacements are very small (less than 10 feet). It was anticipated that the small subsurface fault displacements might create slight lithologic or hydrologic variations on either side of the fault. Variations in electrical properties caused by lithologic or hydrologic differences, as well as fault gouge, should be marked by anomalous resistivity profiles. Consequently, resistivity profiles might provide another method for predicting and mapping faults.

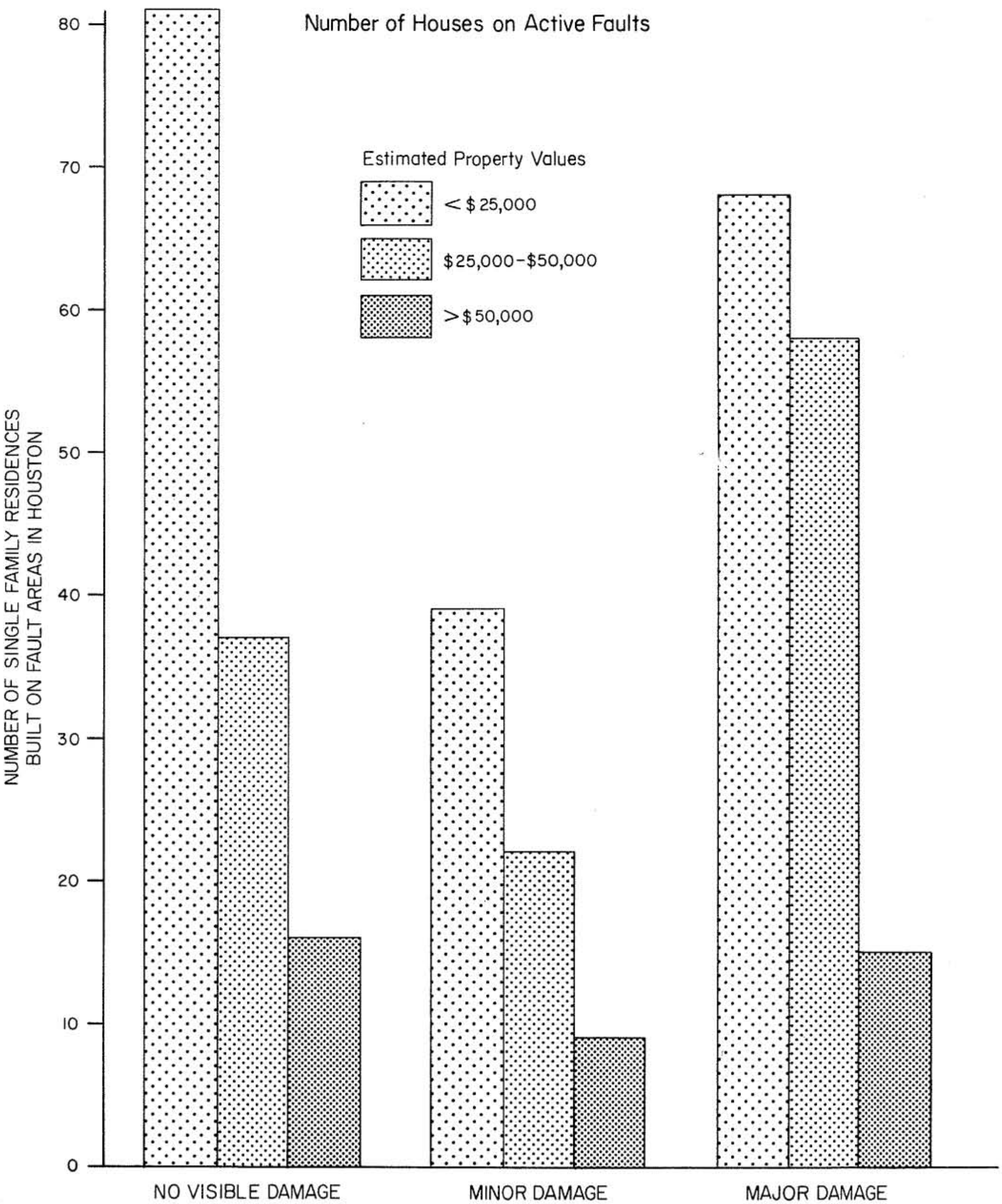

Figure 1. Number of houses on active faults.

Like other techniques for fault identification, resistivity profiling alone cannot confirm the presence or absence of a surface fault. When used in conjunction with other techniques, however, a resistivity profile serves as additional evidence to verify the presence or absence of these costly natural hazards.

RESISTIVITY PROFILING

Earth resistivity is a measurement of the apparent resistivity of geologic materials. Resistivity (ρ) is a constant of proportionality that relates electrical resistance (R) to the length (L) and cross-sectional area (A) of the conducting material:

$$R = \rho \frac{L}{A} \tag{1}$$

According to Ohm's law, resistance is given by

$$R = \frac{\Delta U}{I} \tag{2}$$

where ΔU is the potential difference across the resistance, and I is the electrical current through the resistance.

By combining equations (1) and (2),

$$\rho = \frac{A}{L} \frac{\Delta U}{I} \tag{3}$$

In resistivity measurements, an electrical field is generated between two current electrodes. The voltage drop or potential (ΔU) is measured between two additional electrodes (fig. 2). The fraction $\frac{A}{L}$ in equation (3) is termed the *geometric factor.* In the Wenner array, the electrode array used for this study, four electrodes are equally spaced, the distance between electrodes being a. In this array, $2\P a$ is equivalent to $\frac{A}{L}$. The resistivity equation for the Wenner array then reads

$$\rho_W = 2\P a \frac{\Delta U}{I} \tag{4}$$

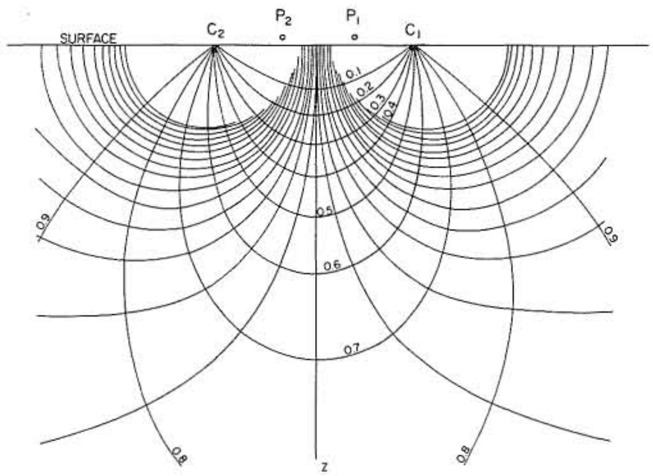

Figure 2. Electrical current and potential field generated between electrodes C_1 and C_2. Potential field measured between P_1 and P_2. Electrodes in Wenner configuration. Modified from Van Nostrand and Cook (1966, p. 31).

If resistivity measurements are made across an infinite volume of homogeneous and isotropic materials, the computed ρ is a true resistivity value. Most geologic materials, however, are anisotropic and heterogeneous. Computed ρ for heterogeneous material is an approximation and is often referred to as apparent resistivity. In this study the term *resistivity* will be used in the context of apparent rather than true resistivity.

Resistivity values range from less than 3 ohm-meters for clays and sands saturated with saline water to several thousand ohm-meters for dry basalts or sand and gravel (Zohdy and others, 1974). Apparent resistivity for Pleistocene and Recent sediments of the Texas Coastal Zone ranges from 3 ohm-meters to 40 ohm-meters (based on the results of this study).

The depth of penetration of the electrical current is approximately equal to the a spacing (Zohdy and others, 1974). An array with an a spacing of 25 feet will be measuring the averaged resistivity of the subjacent geologic material to a depth of 25 feet. Resistivity measurements with an a spacing of 100 feet will be determining average resistivities for subsurface materials to a depth of 100 feet.

Resistivity measurements along a traverse with a constant a spacing are referred to as *resistivity profiling* and measure lateral variations of earth resistivity. Resistivity measurements conducted using an increasing a spacing are known as *resistivity soundings* and measure variations in resistivity with depth. For a more thorough discussion of the theory of resistivity measurements, refer to Zohdy and others (1974) and Van Nostrand and Cook (1966).

RESISTIVITY PROFILING ACROSS SURFACE FAULTS

As early as 1934 Hubbert (1934) and Hubbert and Weller (1934) used surface resistivity measurements to identify faults in Illinois. Since then the technique has developed into a tool often used for fault identification (Van Nostrand and Cook, 1966). Two types of profiles have been recognized where measurements have been made across faults. First, faults separating different lithologies exhibit resistivity profiles characterized by a rapid change at the fault (fig. 3). Tagg (1930), assuming Wenner configuration, calculated theoretical resistivity profiles across a vertical fault separating different lithologies (fig. 3). With increased differences in resistivity (k) across a fault, the resistivity profile steepens at the fault. Rothe and Rothe (1952) computed a theoretical resistivity profile across a known fault and then measured the apparent resistivities across it and observed a positive correlation (fig. 4). Second, faults with gouge material in the fault zone, but with similar lithologies on either side of the fault, exhibit resistivity profiles with marked peaks or troughs at the fault and similar resistivity values on either side (fig. 5). Resistivity profiles across faults that dip steeply through geologic units exhibiting homogeneous resistivity values on either side are analogous to resistivity profiles that cross vertical, perfectly conducting (or insulating) planes. A profile across a perfectly insulating plane (fig. 5) displays a W-shaped curve with a high resistivity value at the plane (Van Nostrand and Cook, 1966). Johnson (1934) found that with an increased a spacing, the W-shaped profile flattens (fig. 6). Resistivity profiles across a perfectly conducting plane produce a similar W-shaped profile, but the resistivity ratio $\frac{\rho_a}{\rho}$ does not exceed 1.0 (fig. 5). Profiles across perfectly conducting or insulating planes are analogous to resistivity profiles across narrow dikes or brecciated zones.

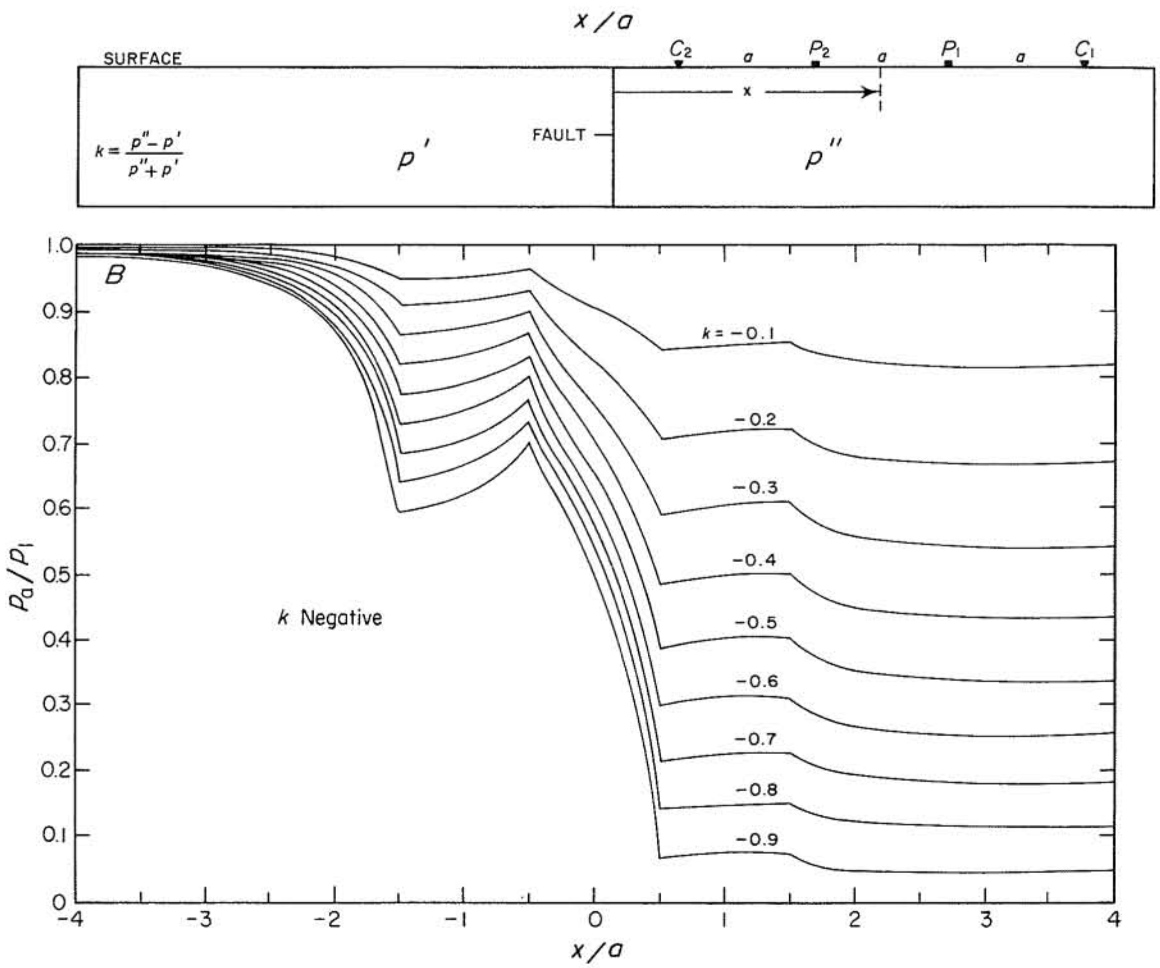

Figure 3. Theoretical horizontal resistivity profiles across a vertical fault, Wenner configuration. Measured apparent resistivity is ρ_a; p' and p'' are theoretical resistivity values. Modified from Tagg (1930) by permission of Mining Magazine.

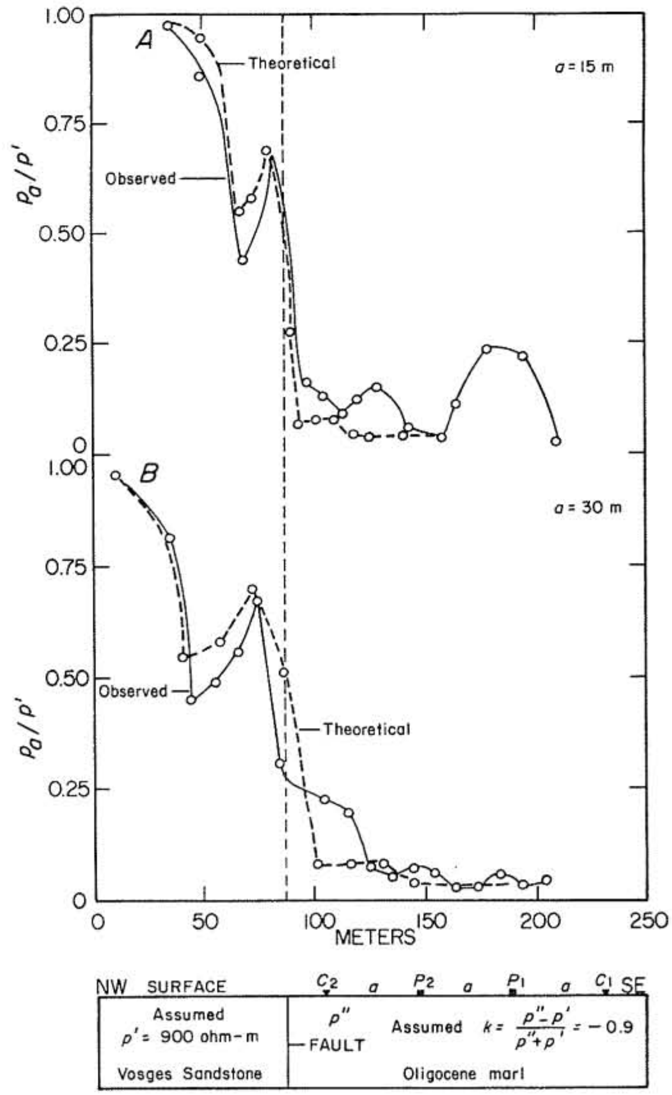

Figure 4. Comparison of observed and theoretical horizontal resistivity profiles across a vertical fault with Wenner configuration (from Rothe and Rothe, 1952).

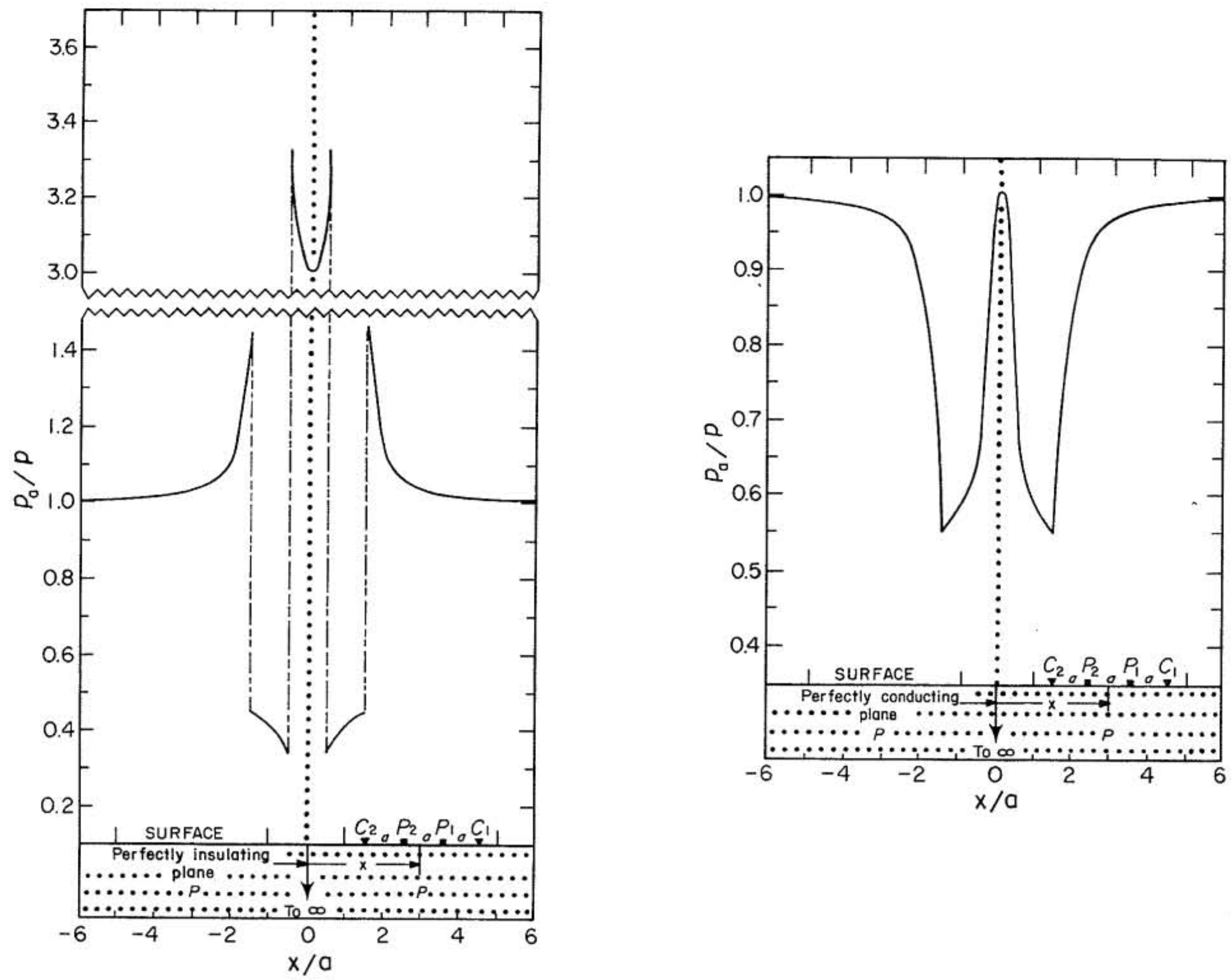

Figure 5. Theoretical horizontal resistivity profiles across perfectly conducting and insulating plane, Wenner configuration. Adopted from Van Nostrand and Cook (1966). Measured apparent resistivity is ρ_a; p' is theoretical resistivity value.

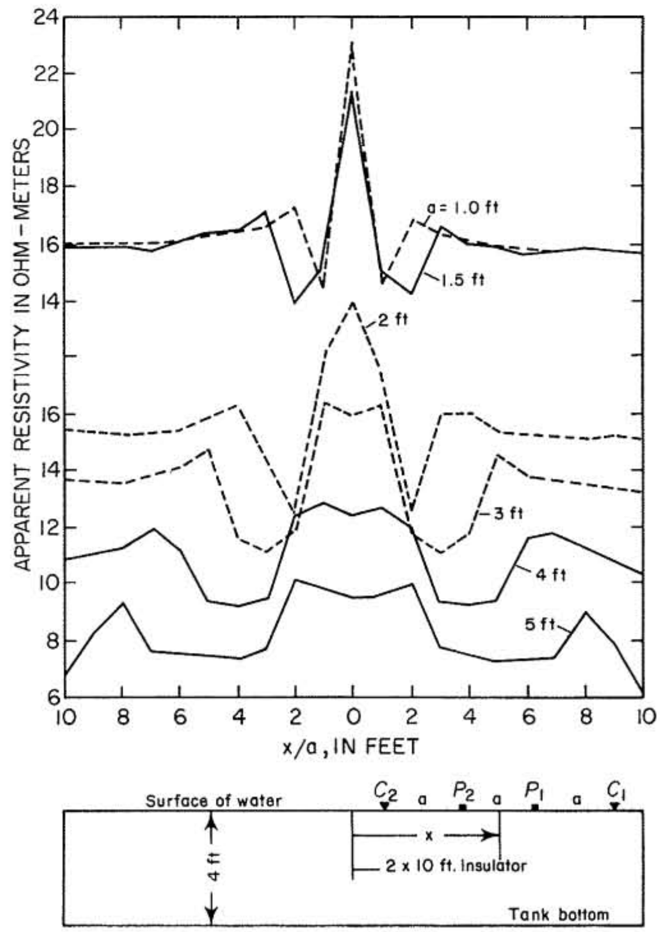

Figure 6. Results of model study of horizontal resistivity profiles across a vertical insulating sheet by increasing a spacing. Modified from Johnson (1934). Copyright by American Institute of Mining Engineers.

RESISTIVITY PROFILING ACROSS SURFACE FAULTS AND LINEATIONS IN THE GREATER HOUSTON AREA

Surface Faults

Horizontal resistivity across 10 faults and 2 lineations in the Texas Coastal Zone was measured using a Wenner configuration. Measurements were made in the summer of 1976 and winter of 1977 using a truck-mounted resistivity meter provided by the Texas Water Development Board. Data from 1976 and 1977 are considered reliable because input current was kept constant, and all readings were replicated.

Resistivity profiles displaying significant resistivity anomalies were recorded at the Baytown fault, Hitchcock fault, Long Point fault, Library fault at Ellington Air Force Base, Clinton fault, and Iowa Colony fault (fig. 7, locations 1-6, respectively). The resistivity profile across the Eureka Heights fault (fig. 7, location 7) showed no significant anomaly. Resistivity profiles across aerial photographic lineations were moderately successful in delineating the feature in the field.

Two types of resistivity profiles across faults have been recognized: (1) profiles exhibiting different resistivities on either side of the fault, and (2) profiles exhibiting a resistivity increase at the fault but with similar resistivity values on either side. The Baytown fault, Hitchcock fault, and Long Point fault are characterized by the first type of profile. Faults characterized by the second type of profile are the Library fault (Ellington Air Force Base), the Clinton fault, the Iowa Colony fault, and Barbers Hill lineation.

Type 1 Faults

The first type of resistivity profile, characterized by materials of different resistivities, is shown by the Baytown fault (fig. 8). Resistivity values across the Baytown fault (location 1, fig. 7) double from the downthrown to the upthrown side. The fault is located at the top of an abrupt increase in resistivity. Profiles with a spacings of 25 feet and 50 feet both show resistivity anomalies. Both profiles exhibit a resistivity peak where the fault scarp bisects the P_1P_2 line.

A resistivity profile (a = 25 feet) across the Hitchcock fault (location 2, fig. 7) displays a profile (fig. 9) similar to that of the Baytown fault (fig. 8). Resistivity values are approximately twice as great on the upthrown side as on the downthrown side. A resistivity peak occurs where the fault scarp intersects $\frac{P_1P_2}{2}$.

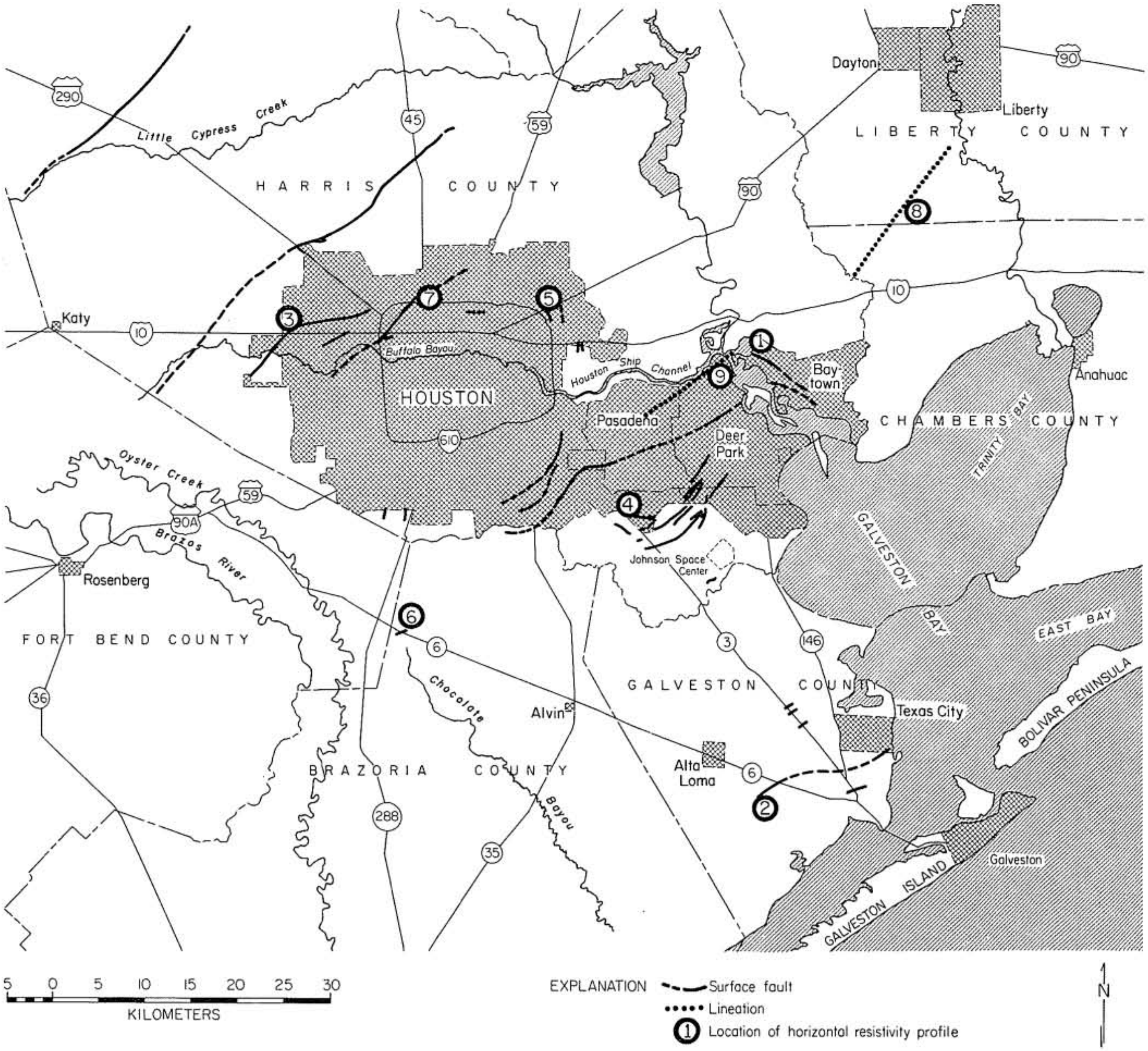

Figure 7. Location map of horizontal resistivity surveys across active faults and aerial photographic lineations.

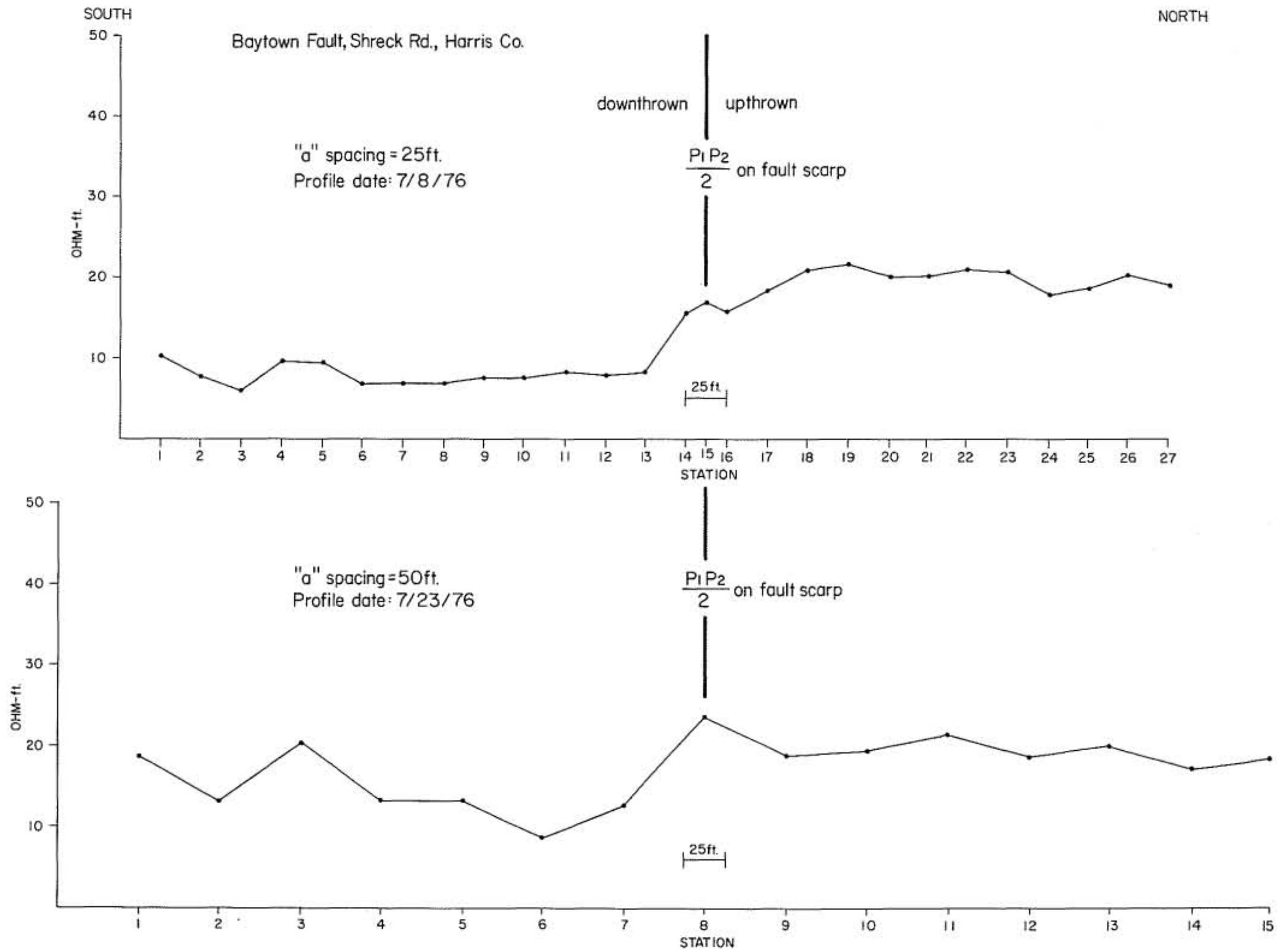

Figure 8. Resistivity profiles across Baytown fault at *a* spacings of 25 and 50 feet. Location 1 on figure 7.

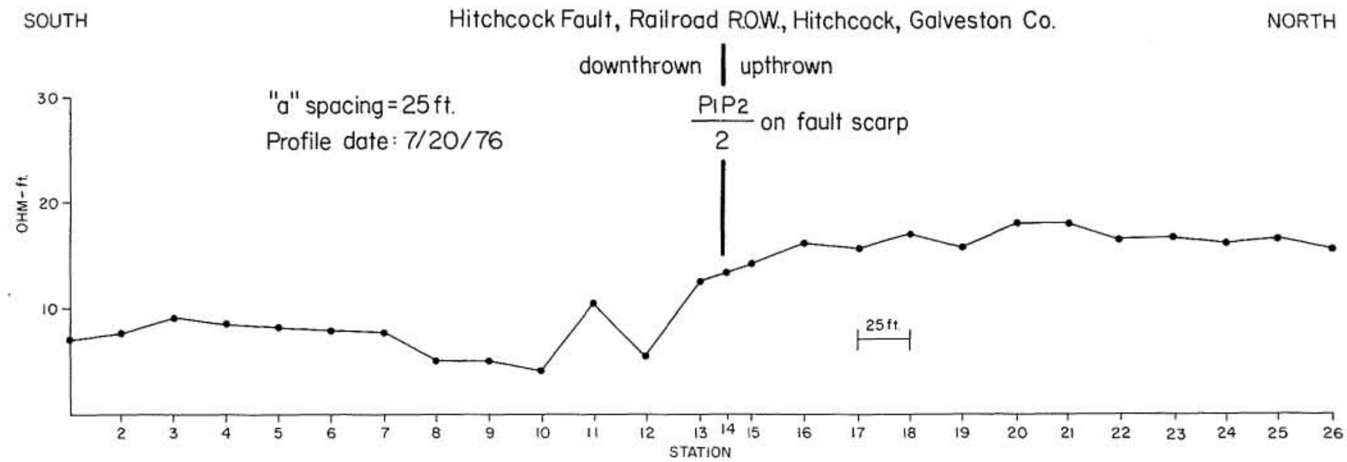

Figure 9. Resistivity profile across Hitchcock fault. Location 2 on figure 7.

A resistivity profile (a = 25 feet) (fig. 10) across the Long Point fault (location 3, fig. 7) is similar to the Baytown and Hitchcock profiles. Resistivity values are approximately 30 percent greater on the upthrown side. A resistivity peak occurs where the fault scarp intersects $\frac{P_1P_2}{2}$.

The topographic escarpments along the Baytown, Hitchcock, and Long Point faults coincide approximately with the top of the first significant sharp rise of values on resistivity profiles. With the Wenner configuration, the faults affect the electrical field in a much wider region. These profiles show the effect of the fault before the C_1 or C_2 electrodes are across the fault. This phenomenon should be expected. Based on figure 3 (from Tagg, 1930), the profile on the high-resistivity side of a fault shows the effect of the fault at a distance of $3 \frac{x}{a}$ (with an a spacing equaling 25 feet, the C_1 electrode will be 37.5 feet from the fault). On the low-resistivity side of the fault, the profile first shows the effect of the fault at a distance of $1.5 \frac{x}{a}$ (with an a spacing equaling 25 feet, the C_1 electrode will be 12.5 feet from the fault).

Lower resistivity measurements occur on the downthrown side of the three faults, perhaps because the water table is closer to land surface or because the soil moisture content is higher on the downthrown side. Sag ponds are common on the downthrown side of many of the active faults. Land surface on the downthrown side of the Baytown fault is about sea level, whereas elevation of the upthrown side is about 3 to 4 feet above sea level. The upthrown side supports a healthy hardwood forest, whereas on the downthrown side the forest has been killed by either brackish surface-water flooding from Galveston Bay or a near-surface water table. Lower resistivity values should be expected on the downthrown side of the Baytown fault. No sag ponds are evident along the Hitchcock and Long Point faults, but the unsaturated zone on the downthrown side may have a higher moisture content and subsequently a lower resistivity.

Type 2 Faults

The second type of resistivity profile observed across a growth fault exhibits high resistivity values at the fault and lower resistivity values on either side. This type of profile is best characterized by horizontal profiles across the Library fault at Ellington Air Force Base (location 4, fig. 7). The escarpment of the Library fault can be traced for approximately 2 km (Clanton and Amsberry, 1976).

Fisher and others (1972) mapped a distributary sand channel through the Ellington area, and the surface and shallow-subsurface lithology is the same on both

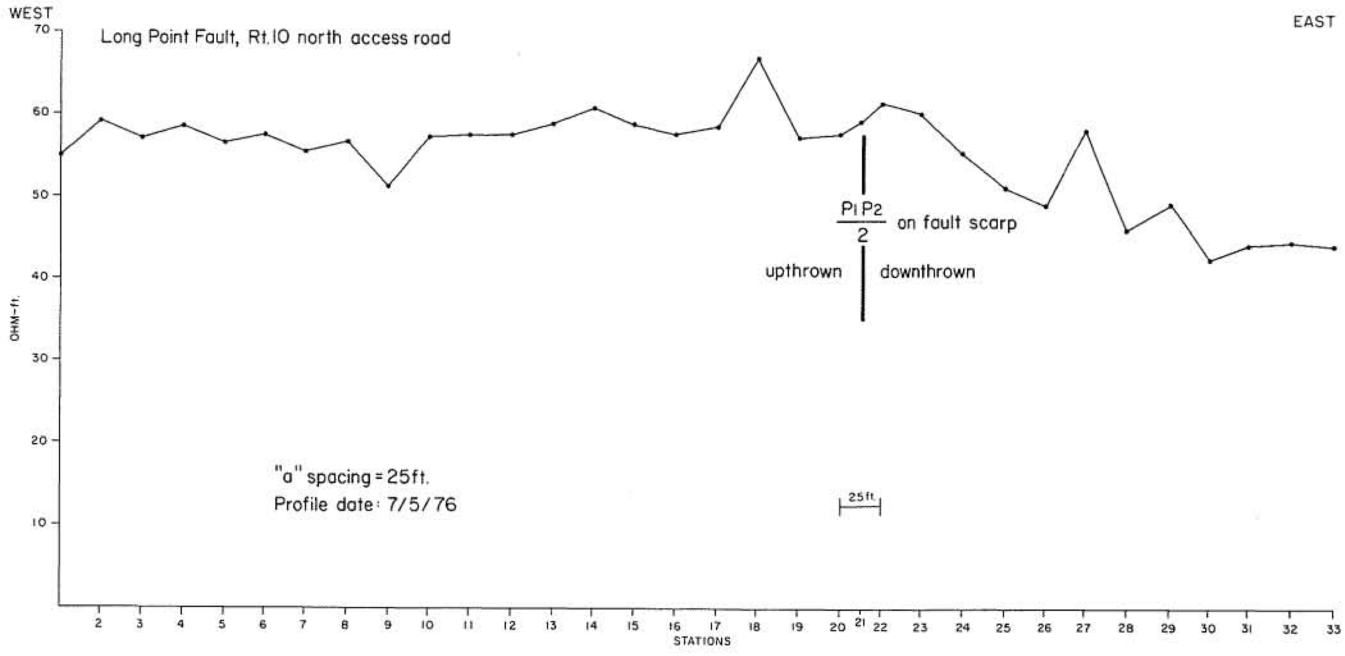

Figure 10. Resistivity profile across Long Point fault. Location 3 on figure 7.

sides of the Library fault. A sand pit operation approximately one-half mile north of the fault in the channel complex exposed at least 50 feet of sand. An 8-foot-deep surface trench across the fault exposed a high sand facies (fig. 11a) with no offsets of discrete lithologic beds like those observed in the trench across the Battleground fault, La Porte, Texas (fig. 11b).

Three resistivity profiles with a spacings of 25 feet, 50 feet, and 100 feet show increased resistivity at the fault and decreased values on either side (fig. 12). The profiles with 25-foot and 50-foot a spacings should have penetrated only geologic material of sand facies.

The horizontal resistivity profile with the a spacing of 25 feet demonstrates a significant increase in resistivity (more than 50 percent) and a W-shaped signature at the fault. With the 50-foot a spacing there is approximately a 30-percent increase in resistivity at the fault, but the W-shaped profile still defines the fault. With the 100-foot a spacing, resistivity increases 20 percent at the fault, and no W-shaped signature is recorded. Johnson (1934) demonstrated a similar widening and flattening of the W-shaped resistivity profile as the a spacing is increased across a high-resistivity boundary (fig. 6).

These type 2 resistivity profiles are similar in shape to profiles across dikes, brecciated rocks, and mineralized zones (see Van Nostrand and Cook, 1966, for examples). The increased resistivity at the fault indicates physical alteration of the sediments (gouge zones) associated with the fault.

Horizontal resistivity profiles across the Clinton and the Iowa Colony faults show increased resistivity at the fault and decreased values on either side. Resistivity increases by 33 percent (fig. 13) at the Clinton fault (location 5, fig. 7) and by 15 percent (fig. 14) at the Iowa Colony fault (location 6, fig. 7). These resistivity anomalies are subtle, but they do suggest a physical alteration of the sediments in the fault zone.

The horizontal resistivity profile across the Eureka Heights fault is inconclusive in demonstrating a change in resistivity at the fault (fig. 15). This survey was conducted along the access road to Interstate Highway 610 (the loop around Houston). Construction of the highway may have homogenized the shallow subsurface during road-grading operations and eliminated the resistivity break.

Figure 11a. Trench across Library fault, Ellington Air Force Base. Note thickening of soil profile on downthrown side of fault. No fault plane surface evident.

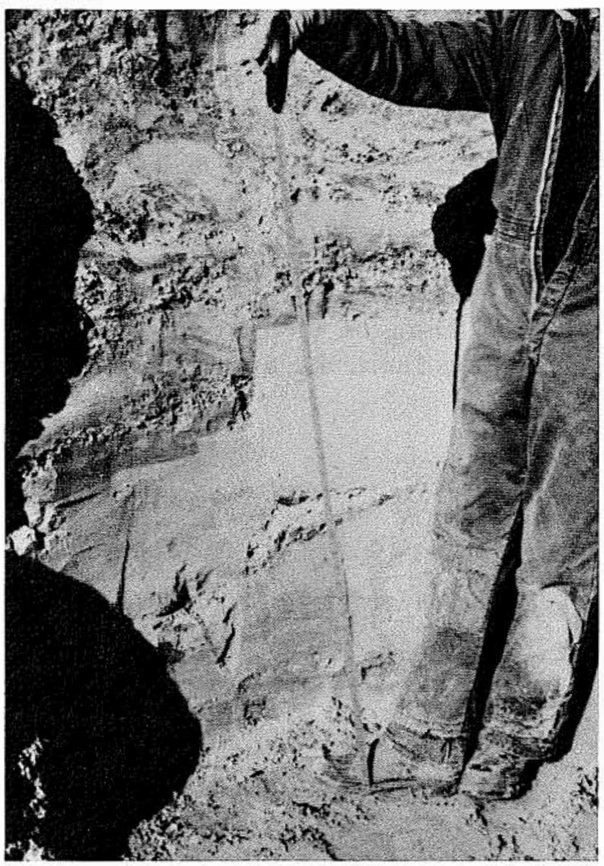

Figure 11b. Trench across Battleground fault, La Porte, Texas. Note offset of sand beds. Approximately 14 inches of displacement. Photograph courtesy Wilbur Evans.

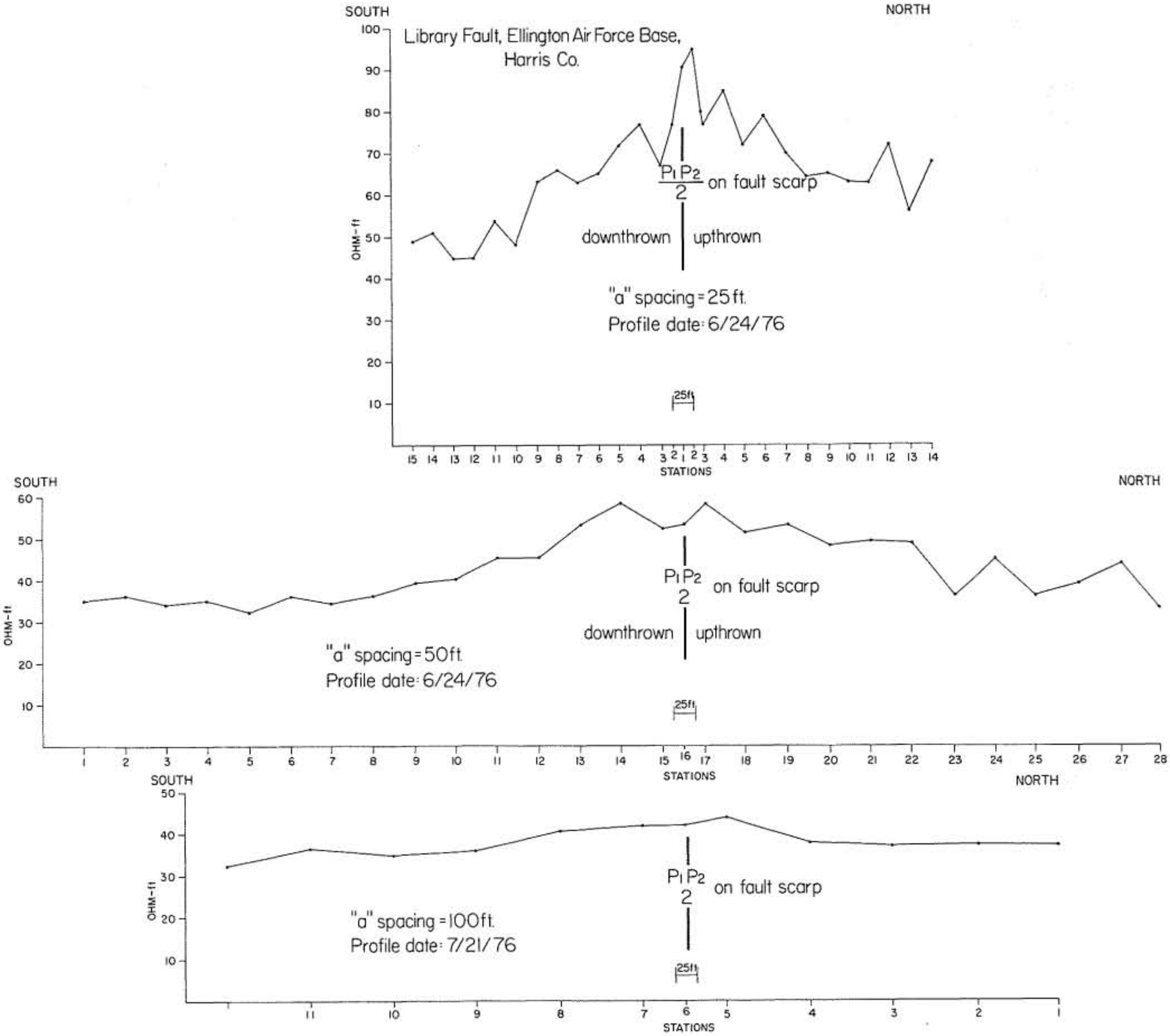

Figure 12. Resistivity profiles across Library fault, Ellington Air Force Base at *a* spacings of 25, 50, and 100 feet. Figure 11a is a trench across this fault. Location 4 on figure 7.

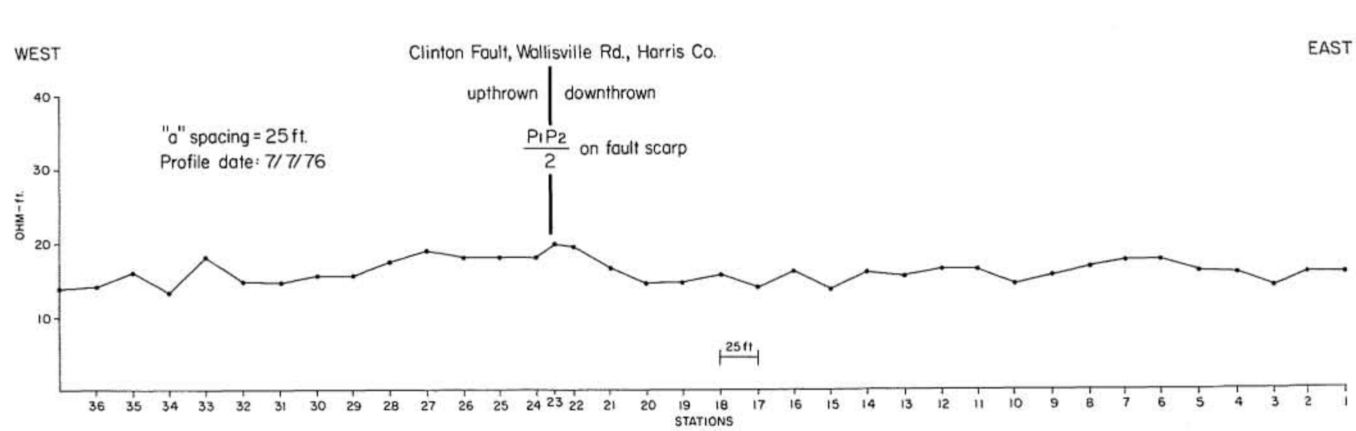

Figure 13. Resistivity profile across Clinton fault. Location 5 on figure 7.

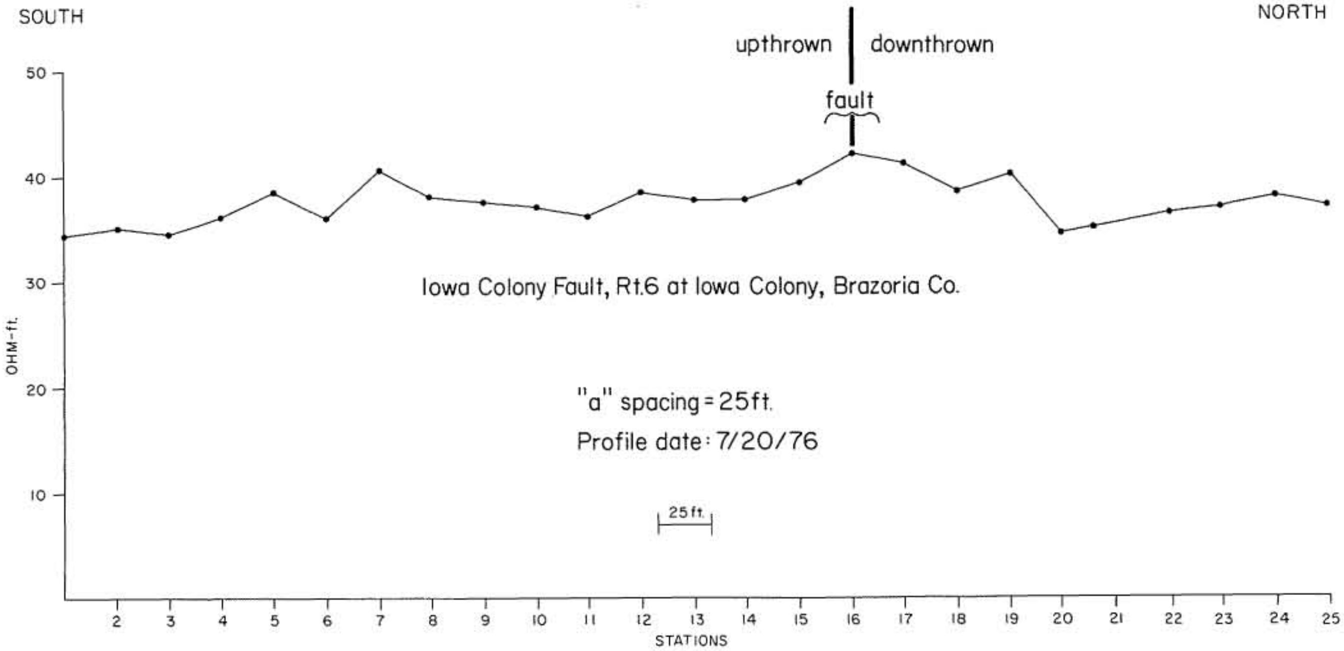

Figure 14. Resistivity profile across Iowa Colony fault. Location 6 on figure 7.

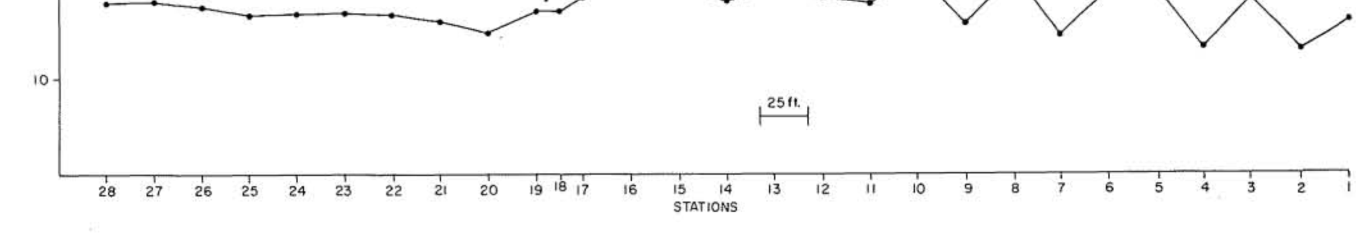

Figure 15. Resistivity profile across Eureka Heights fault. Location 7 on figure 7.

Lineations

Aerial photographic lineations in the Texas Coastal Zone commonly are the surficial expression of growth faults (Kreitler, 1976). Resistivity traverses were conducted across two lineations to determine if this technique would confirm a structural origin of the lineation. The Barbers Hill lineation, north of Mount Belview on State Highway 146 in Chambers County (east of Houston), Texas, and the San Jacinto lineation, through the reflection pool in San Jacinto Monument State Park, were chosen for evaluation.

The Barbers Hill lineation (location 8, fig. 7), which was mapped initially on black-and-white aerial photographic mosaics, is coincident with a color-infrared aerial photographic lineation and the surface trace of an extrapolated subsurface fault. In the field, a vegetation change marks the lineation. At the location of the resistivity survey, the lineation is within a Pleistocene distributary channel, and the surficial geology appears to be similar on either side of the lineation.

The resistivity profile exhibits an increase of approximately 50 percent in resistivity at the lineation (fig. 16) and lower but similar resistivity values on either side. The resistivity profile resembles the profile across the Library fault at Ellington Air Force Base. The increased resistivity implies a physical alteration of the substrate beneath the lineation and a structural origin of the lineation.

Evidence for a fault through the San Jacinto Monument Reflection Pool is (1) an aerial photographic lineation, (2) a rapid increase in subsidence down the length of the pool toward the monument, and (3) asphalt patches on the access road around the pool (Kreitler, 1976). Horizontal resistivity profiles across the lineation (location 9, fig. 7) demonstrate very slight resistivity deflections (fig. 17). These breaks are insufficient evidence to verify a surface fault.

HORIZONTAL RESISTIVITY PROFILING-- A TOOL FOR IDENTIFYING SURFACE FAULTS

Horizontal resistivity profiling with a Wenner array is another technique to identify surface faults along the Gulf coast. Like other techniques, it is not always successful. Faults such as the Baytown, Hitchcock, or Library exhibit significant resistivity deflections. Faults such as the Iowa Colony and Clinton show subtle resistivity anomalies. Resistivity profiles across lineations proved only moderately successful.

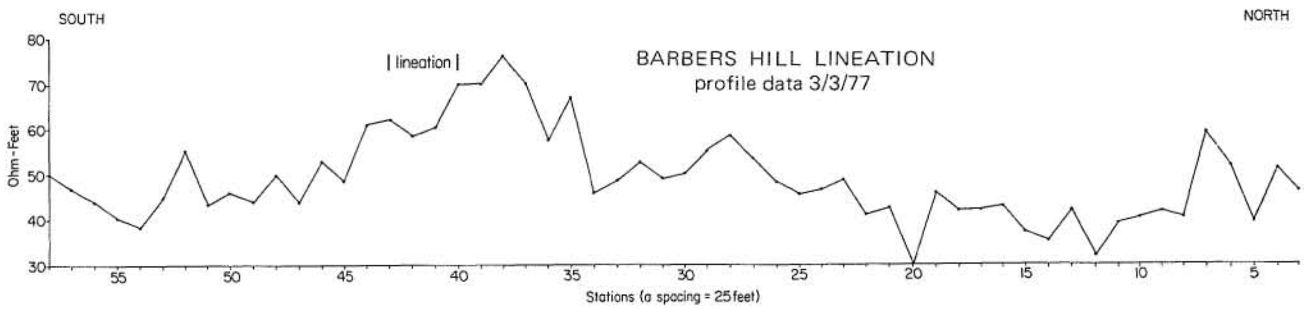

Figure 16. Resistivity profile across Barbers Hill lineation on State Highway 146 north of Mount Belview, Texas. Location 8 on figure 7.

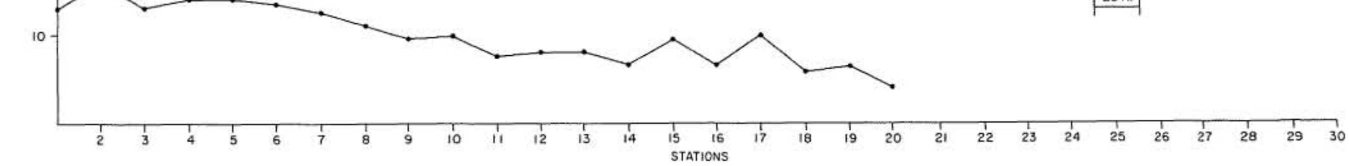

Figure 17. Resistivity profile across San Jacinto lineation at San Jacinto Monument State Park. Location 9 on figure 7.

An a spacing of 25 feet is recommended. Wider spacings reduce the resistivity anomalies. Precise fault location could not be determined by using a station spacing of 25 feet; faults could be located more precisely by maintaining the 25-foot a spacing but decreasing the station spacing to 5 or 10 feet.

PHYSICAL CHARACTERISTICS OF SURFACE FAULTS THAT MAY BE INFERRED FROM HORIZONTAL RESISTIVITY PROFILES

Resistivity profiles across the Library fault at Ellington Air Force Base suggest that a zone of physical alteration of sediments exists along the fault. Formation of gouge along a fault plane is common. Tectonic faults across alluvial basins in California have created gouge zones of sufficiently low permeability that ground water can be stored on the upthrown side of the fault (Williams, 1970). Faults have compartmentalized sandstone beds in the Wilmington Oil Field, forming barriers to fluid migration and pressure communication (Mayuga, 1970). Decreased permeability across the faults of the Texas Gulf coast is a definite possibility. Conversely, increased permeability within the fault zone might cause increased resistivity if ground water with lower total dissolved solids were migrating up the fault planes.

The resistivity profile at the Library fault defines a relatively wide zone of alteration. The zone of highest resistivity is approximately 200 feet wide. A 400-foot-wide zone of increased resistivity from background levels indicates that a wide zone of sediment is affected on either side of the fault.

ACKNOWLEDGMENTS

The authors are indebted to L. F. Brown, Jr., A. R. Gregory, R. L. Andersen (Bureau of Economic Geology, The University of Texas at Austin) and Dan Muller (Texas Department of Water Resources) for their critical review of this manuscript, and to Doug Ratcliff and Russell Lewis (Bureau of Economic Geology) and U. S. Clanton (National Aeronautics and Space Administration) for their field assistance. The technical assistance of Dan Muller and the use of the Texas Water Development Board's truck-mounted resistivity meter were greatly appreciated. This investigation was sponsored by the U. S. Geological Survey, Department of Interior, under USGS Grant No. 14-08-0001-G144.

REFERENCES

Clanton, U. S., Jr., and Amsberry, D. L., 1976, Active faults in southeastern Harris County, Texas: Environmental Geology, v. 1, no. 3.

Fisher, W. L., McGowen, J. H., Brown, L. F., Jr., and Groat, C. G., 1972, Environmental Geologic Atlas of the Texas Coastal Zone--Galveston-Houston Area: The University of Texas at Austin, Bureau of Economic Geology, 91 p.

Hubbert, M. K., 1934, Results of earth resistivity on various geologic structures in Illinois: Transactions of the American Institute of Mining Metallurgical and Petroleum Engineers, v. 110, p. 9-39.

Hubbert, M. K., and Weller, J. M., 1934, Location of faults in Hardin County, Illinois, by the earth resistivity method: Transactions of the American Institute of Mining Metallurgical and Petroleum Engineers, v. 110, p. 40-48.

Johnson, H. N., 1934, Discussion of paper by M. K. Hubbert, 1932, *in* Transactions of the American Institute of Mining Metallurgical and Petroleum Engineers, v. 110, p. 30-31.

Kreitler, C. W., 1976, Lineations and faults in the Texas Coastal Zone: The University of Texas at Austin, Bureau of Economic Geology Report of Investigations 85, 32 p.

Mayuga, M. N., 1970, Geology and development of California's giant--Wilmington Oil Field: American Association of Petroleum Geologists, Memoir no. 14, Geology of giant petroleum fields, p. 158-184.

Rothe, E., and Rothe, J. P., 1952, Prospection geophysique: Paris, Gauthier-Villars, v. 2, p. 185-486.

Tagg, G. F., 1930, The earth resistivity method of geophysical prospecting: Some theoretical considerations: Mining Magazine, v. 43, no. 3, p. 150-158.

Van Nostrand, R. G., and Cook, K. L., 1966, Interpretation of resistivity data: U. S. Geological Survey Professional Paper 499.

Williams, D. E., 1970, Use of alluvial faults in the storage and retention of ground water: Ground Water, v. 8, no. 5, p. 25-29.

Zohdy, A. D. R., Eaton, G. P., and Mabey, D. R., 1974, Application of surface geophysics to ground-water investigations: U. S. Geological Survey, Techniques of Water-Resources Investigations, Book 2, Chap. D1, 116 p.